

Estimating the location of the hook-wire used in breast-conserving surgery using a magnetometer

Oiendrila Bhowmik Debnath¹⁾, Akihiro Kuwahata¹⁾, Yuki Sunaga²⁾, Shinichi Chikaki¹⁾, Miki Kaneko¹⁾, Moriaki Kusakabe³⁾⁴⁾, and Masaki Sekino^{1)2)a)}

¹⁾ Department of Electrical Engineering and Information Systems, Graduate School of Engineering, the University of Tokyo, Tokyo, Japan

²⁾ Department of Bioengineering, Graduate School of Engineering, the University of Tokyo, Tokyo, Japan

³⁾ Matrix Cell Research Institute Inc., Ibaraki, Japan

⁴⁾ Research Center for Food Safety, Graduate School of Agricultural and Life Sciences, the University of Tokyo, Tokyo, Japan

^{a)} Corresponding author: Masaki Sekino, sekino@g.ecc.u-tokyo.ac.jp

In the surgical treatment of nonpalpable breast lesions, such as in early-stage cancer, a hook-wire is inserted into the lesion as a marker to enable surgeons to excise the tissue, along with the hook-wire, with a good margin. However, a benchmark technique for intraoperatively determining whether the excised tissue has an appropriate margin around the lesion has not yet been established. In this study, a method for locating a ferromagnetic stainless steel hook-wire inside the excised tissue using a magnetometer is proposed. The magnetometer is placed around a phantom along with the hook-wire at varied locations to map the magnetic field distribution. The three-dimensional coordinates of hook-wire are obtained by executing an optimization algorithm. The experimental results indicate that the location of the hook-wire is successfully obtained. Based on the information regarding the margin around the hook-wire, the surgeon can immediately evaluate the risk of whether some cancer cells still remain in the body.

I. INTRODUCTION

Breast cancer screening using mammography has enabled its early detection, thus resulting in desirable treatment outcomes.¹ Often, the recommended course of treatment for breast cancer detected at stages I and II is breast-conserving surgery, whereby a surgeon removes the tumor, along with a certain margin, while leaving as much normal tissue as possible. In such surgeries, some surrounding healthy tissue is also excised to confirm that all the cancer tissue was removed.^{2,3} This is important for circumventing any local recurrence of tumor.⁴ Early-stage cancers may not be palpable, and therefore, a small implantable device can function as crucial a guide to mark the lesion for excision.^{5,6} A hook-wire is a typical marker device that is used globally. Before surgery, a hook-wire is inserted into the lesion using ultrasound imaging. Based on visual approximation, a margin is drawn around the area of insertion of the hook-wire. Subsequently, the surgeons operate on the entire suspicious area, including the margin. After the tissue is excised, it is conventionally sent for X-ray analysis to check the two-dimensional image of the hook-wire location and the margin around the hook-wire.³ If the margin is insufficient, reexcision is performed to avoid the risk of leaving some cancer cells in the body.⁷ However, inspecting the three-dimensional position of the hook-wire is crucial when checking the margin.

In this light, this study proposes an alternative method, wherein a commercially-available hook-wire is inserted to mark the lesion, and the magnetization of the hook-wire is measured using a magnetometer^{8,9} at the surface of the tissue specimen. The location of the hook-wire and margin around hook-wire can be determined by estimating the three-dimensional location of the tip of the hook-wire.

II. MATERIALS AND METHODS

A. Experimental Setup

Figure 1 shows a schematic of the experimental setup comprising the phantom, magnetometer, and hook-wire. The

magnetometer was equipped with a neodymium permanent magnet and two Hall sensors, both inside the cylindrical tip of the magnetometer.⁸ The sensors were placed along the symmetrical axis of the cylindrically shaped magnet.

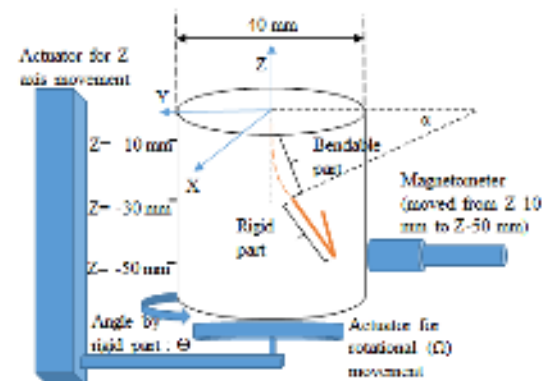


FIG. 1. Measurement setup showing the hook-wire and the magnetometer. Angle caused by hook-wire's rigid part is θ . The distance between the surface of the phantom and the magnetometer was kept constant. The magnetometer was located along the x-axis ($\Omega = 0$) at the beginning of the measurement.

The hook-wire used herein was manufactured by Argon Medical Devices (Breast localization needle) and is commercially available. It typically consists of two parts, namely, upper and lower parts. The lower part is rigid and designed in the shape of a hook, whereas the upper part is bendable. The length of the manufactured hook-wire was 300 mm.

In this study, the hook-wire was placed inside a phantom, and the bendable part of the hook was cut to reduce the overall length of the hook-wire to 50 mm, as shown in Fig. 2. The position of the hook-wire had three degrees of freedom

defined by α , θ , and ψ , as shown in Fig. 3. Table 1 presents the variations in these three parameters. Phantoms were manufactured for each combination of the three parameters listed in Table 1.

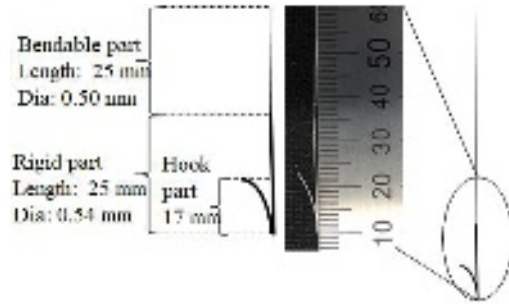


FIG. 2. Structure of the 50-mm hook-wire showing the dimensions of the rigid and bendable parts.

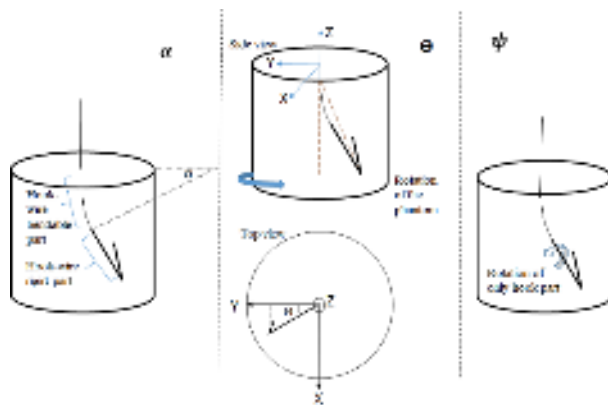


FIG. 3. Parameters to be varied to make the phantoms: α shows the angle of the bendable part of the hook-wire, θ shows the orientation angle of the hook-wire with respect to the x-axis, and ψ shows the rotation angle along the rigid part of the hook-wire inside the phantom.

TABLE I. Parameters for describing the location and orientation of the hook-wire for obtaining reference data using the parameters defined in Fig. 3.

	α (°)	θ (°)	ψ (°)
1	0	0	0
2	5	60	30
3	10	120	60
4	20	180	90
5	30	240	120
6		300	150
7			180
8			210
9			240
10			270
11			300
12			330

In the experiments performed herein, the position of the magnetometer was fixed to avoid any error caused by the earth's magnetic field. Two actuators were used to move the phantom; one was used for the z-axis movement, whereas the other was used for rotational (Ω) movement. The actuator for

the z-axis movement was varied every 10 mm for a total distance of 50 mm, whereas the actuator for the rotational movement was varied every 30° , covering 360° . Thus, the total number of sampling points was $5 \times 12 = 60$ points.

When the phantom containing the hook-wire with surrounding tissue came in close contact to the magnetometer, the permanent magnet induced magnetization in the hook-wire, and the Hall sensor detected the magnetic field generated by the hook-wire.^{8,9} The magnetometer recorded the magnetic field for each of the positions listed in Table 1.

In the experiment, a finite number of points were defined around the phantom at which the magnetic field strengths were measured. To estimate the unknown target parameters α , θ , and ψ from the measured magnetic field, the relationship between the measured magnetic field and these parameters were modeled using a mathematical function, as defined in Eq. (1). This equation is based on trilinear interpolation and yields the magnetic field, f_n , at the n -th recording point as a function of the three parameters, namely α , θ , and ψ . The coefficient b_{ijk} was determined using a set of equations expressed in Eq. (2).¹⁰

$$f_n(\alpha, \theta, \psi) = \sum_{(i,j,k) \in \{0,1\}^2} b_{ijk} \alpha^i \theta^j \psi^k, \quad (1)$$

$$\begin{cases} \sum_{(i,j,k) \in \{0,1\}^2} b_{ijk} \alpha_0^i \theta_0^j \psi_0^k = \hat{f}_n(\alpha_0, \theta_0, \psi_0) \\ \sum_{(i,j,k) \in \{0,1\}^2} b_{ijk} \alpha_1^i \theta_1^j \psi_1^k = \hat{f}_n(\alpha_1, \theta_1, \psi_1) \end{cases}, \quad (2)$$

where α_0 , α_1 , θ_0 , θ_1 , ψ_0 , and ψ_1 denote any subsequent values in Table 1. In equation (1), the ranges of α , θ , and ψ satisfy $\alpha_0 \leq \alpha \leq \alpha_1$, $\theta_0 \leq \theta \leq \theta_1$, and $\psi_0 \leq \psi \leq \psi_1$, respectively. Here i , j , and k are either 0 or 1. Given that Eq. (1) is based on a trilinear interpolation, \hat{f}_n is the measured value when α , θ , and ψ are identical to the values listed in Table 1. Otherwise, f_n returns a value estimated from the interpolation. This mathematical model was used in the optimization algorithm discussed in the next section.

B. Algorithm for Determining Target Parameters

This section explains the algorithm used to optimize the values of α , θ , and ψ to locate the hook-wire. The stochastic gradient descent optimization algorithm was used to optimize the parameters. The main purpose of this step was to reduce the function $F(\alpha, \theta, \psi)$, as described in Eq. (3).

$$F(\alpha, \theta, \psi) = \sum_{n=1}^{N=60} (f_n(\alpha, \theta, \psi) - B_n)^2, \quad (3)$$

where $f_n(\alpha, \theta, \psi)$ is the reference magnetic field defined in equation (1), and B_n is the magnetic field measured from a sample whose hook-wire has an unknown position. Gradient descent is an iterative algorithm that begins from a random point on a function and travels down its slope in steps until it reaches the minimum. Herein, optimization was performed on the test dataset to obtain the optimal combination of α , θ , and ψ . The gradient of the objective function (Eq. (3)) with respect to each of the three parameters was calculated. Furthermore, as shown in Eq. (4), the step sizes to update each parameter were calculated by multiplying the gradient with the learning rate, ϵ , which was set to be 0.01. The parameters were updated with these step sizes, and this process was repeated until the gradient diminished to an appropriate

amount. This optimization algorithm considered nine initial points, which is sufficient for calculating the minima and determining the target parameters.

$$\begin{pmatrix} \alpha \\ \theta \\ \psi \end{pmatrix}_{m+1} = \begin{pmatrix} \alpha \\ \theta \\ \psi \end{pmatrix}_m - \epsilon \begin{pmatrix} \frac{\partial F}{\partial \alpha} \\ \frac{\partial F}{\partial \theta} \\ \frac{\partial F}{\partial \psi} \end{pmatrix}. \quad (4)$$

The objective of this study was to obtain the three-dimensional location of the tip of the hook-wire in the sample. The values of α , θ , ψ were used to calculate the location of the tip of the hook-wire in the Cartesian coordinate system. In Fig. 4, R is the radius of curvature of the bendable part, R' is the shortest length made by the arc, λ is the length of the arc, x' is the distance between the ends of the bendable part along the x-axis, and z' is the distance in the z-axis owing to only the bendable part. Further, L is the length of the rigid part of the hook-wire, x'' is the distance between the ends of the rigid part on the x-axis, and z'' is the distance on the z-axis made by the same. Therefore, the total lengths made by the entire hook-wire in the x- and z-axes are expressed by Eq. (5).

$$\begin{cases} z = z' + z'' \\ x = x' + x'' \end{cases}. \quad (5)$$

Eq. 6 yields the x-, y-, and z-axis coordinates of the tip of the hook-wire. Thus, the margin of the hook-wire from the sidewall of the phantom or the top wall of the phantom can be calculated, as follows.

$$\begin{cases} z = R \cos(90^\circ - \alpha) + L \sin(90^\circ - \alpha) \\ x = \sqrt{R'^2 - z'^2} + L \cos(90^\circ - \alpha) \\ y = \sqrt{z^2 - x^2} \sin \theta \end{cases}. \quad (6)$$

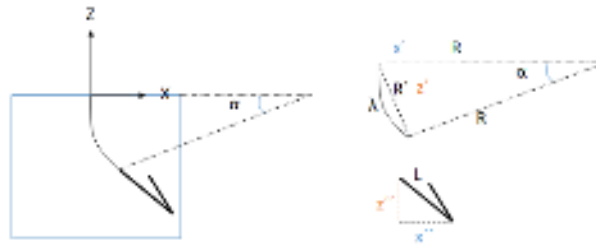


FIG. 4. Bendable and rigid parts of the hook-wire with their respective parameters used to calculate the location of the tip of the hook-wire in Cartesian coordinates.

III. RESULTS AND DISCUSSION

The results of the experiment showed a variation in the magnetic field strength based on the location of the hook-wire. Figure 5(a) shows a schematic of the hook-wire when α is 0° and 30° . Figure 5(b) shows the x-axis value for various values of α . Evidently, when α was 0° (x-axis value at 0), the distance between the magnetometer and hook-wire was 20 mm. Whereas when α was 30° , the x-axis value was 18.2 mm, essentially corresponding to a distance between the magnetometer head and tip of the hook-wire of 1.8 mm. Figure 5(c) shows the variations in the magnetic field strength due to variations in α . A maximum magnetic field strength of $58.7 \mu\text{T}$ was obtained when α was 20° , and it was reduced to $33.2 \mu\text{T}$ when α was increased to 30° . This reduction in the

magnetic field strength was due to a shift in the tip of the hook-wire in the positive direction along the z-axis owing to variations in α . When α was 30° , the tip of the hook-wire moved further in the positive direction, and hence, the magnetic field strength detected by the magnetometer at that point was reduced.

Figure 6(a) demonstrates a case in which the hook of the hook-wire was 180° opposite to the magnetometer head. For these cases, the angle ψ was constant at 180° , whereas α was varied. Figure 6(b) shows the magnetic field variation when the z-axis location of the magnetometer was -50 mm. As the hook part was bent, a variation in magnetic field strength was observed over α variation. A difference in the magnetic field strength of $22 \mu\text{T}$ was observed when α was increased from 20° to 30° . This is because when α was increased, the magnetic field strength increased owing to the proximity of the hook with the magnetometer head.

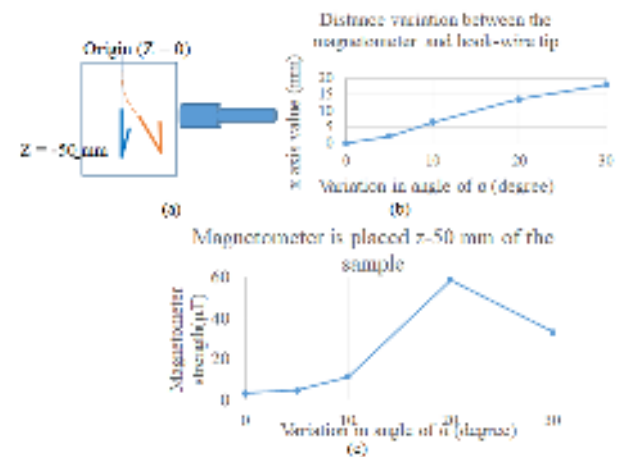


FIG. 5. (a) When the hook-wire orientation, α , increases, the hook-wire comes closer to the head of the magnetometer; (b) distance variation between the magnetometer and hook-wire tip due to variations in α of the bendable part; (c) magnetic field strength data with varying α .

The value of θ was varied to understand its effect on the magnetic field strength, while α and ψ remained fixed. Three values of $\alpha = 0^\circ, 10^\circ, \text{ and } 30^\circ$, were examined, while maintaining ψ as constant at 0° . Figure 7(a) shows the orientation of the hook-wire and the sample with α of $0^\circ, 10^\circ, \text{ and } 30^\circ$. Figure 7(b) shows the magnetic field strength at $\alpha = 0^\circ, 10^\circ, \text{ and } 30^\circ$ while varying θ (0° – 360°). Evidently, when α was 30° , and $\theta = 0^\circ$, the magnetic field strength was at a maximum of $33 \mu\text{T}$. The difference in the value of the magnetic field between $\theta = 0^\circ$ and 180° was approximately $35 \mu\text{T}$ (Fig. 7(b)). By contrast, when α was 0° , the magnetic field strength remained almost the same with the variation in θ because the distance between the tip of the hook-wire and head of the magnetometer did not change.

The optimization algorithm was based on the dependence of the measured magnetic field strength on α , θ , and ψ . To validate the efficacy of optimization algorithm, ten experiments were performed for all of the combination of initial parameters provided in Table 1. In these cases, the

algorithm worked successfully and gave errors of less than 0.5 mm. To establish the efficacy, four black-box experiments were conducted. In these experiments, the hook-wire was placed in a random orientation, which was not previously recorded. In the black-box experiments, the magnetometer recorded one data set (60 sampling points), which was then input to the optimization algorithm.

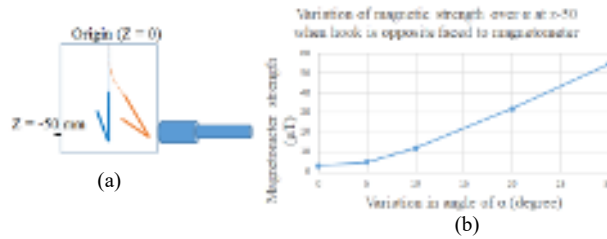


FIG. 6. (a) Hook-wire orientation when α is varied: hook part of the hook-wire was opposite to the magnetometer; (b) magnetic field strength data when α varies for $\psi = 180^\circ$.

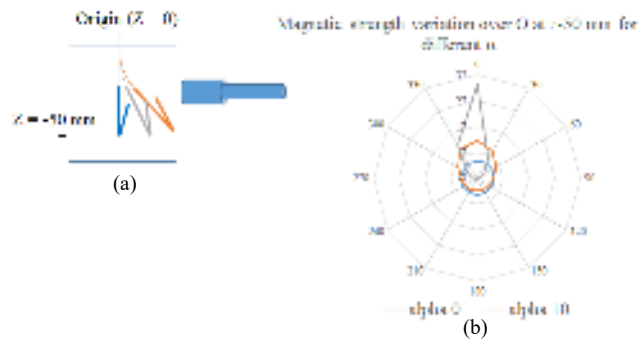


FIG. 7. (a) Hook-wire orientation when α is varied: different colors show the different α variation of 0° , 10° and 30° of the bendable part; (b) magnetic field strength data when α varies as y-axis value changes due to θ variations.

TABLE II. Comparison between the black-box three-dimensional coordinate value (input) and output coordinate value.

Black-box parameters	Input (in mm)			Output (in mm)		
	X	Y	Z	X	Y	Z
Input (α, θ, ψ): $10^\circ, 0^\circ, 0^\circ$ Output (α, θ, ψ): $8.5^\circ, 0^\circ, 0^\circ$	6.58	0	-49.5	6.43	0	-47.3
Input (α, θ, ψ): $20^\circ, 60^\circ, 130^\circ$ Output (α, θ, ψ): $19.2^\circ, 20^\circ, 90^\circ$	13.59	16.3	-48.5	13.28	7.1	-48.09
Input (α, θ, ψ): $10^\circ, 180^\circ, 10^\circ$ Output (α, θ, ψ): $9.8^\circ, 120^\circ, 356^\circ$	6.58	18.3	-49.5	6.4	16.7	-49.4
Input (α, θ, ψ): $5^\circ, 0^\circ, 160^\circ$ Output (α, θ, ψ): $5.1^\circ, 60^\circ, 120^\circ$	2.17	0	-49.8	3.1	14.1	-49.5

Table 2 presents a comparison of the three-dimensional location of the hook-wire input and output data based on four datasets. The average error for the x-, y-, and z-axes were calculated and found to be 0.4 mm, 6.2 mm, and 0.8 mm, respectively. The maximum error of 14.1 mm was observed for the y-axis because the orientation of the hook-wire led to a similar type of dataset in some cases, and the θ variation was comparatively higher in the output. The error was found to be within 2 mm after implementing the optimization algorithm on the provided data for the x- and z-axes. In a previous clinical trial of breast-conserving surgery, the mean size of the lesion was 11.1 mm, ranging from 0 to 33 mm.¹¹ Sizes of surrounding normal tissue largely differ between surgeons. These sizes of lesion suggest that the errors found in this study are in an acceptable range for relatively large lesions. Patients having large lesions can be selected preoperatively using X-ray or ultrasound imaging. Our future work will be to improve further the accuracy of estimation, introducing a multi-point measurement can be effective. This can be realized by implementing a multi-axis sensor in the magnetometer.

IV. CONCLUSION

In this study, a magnetometer was employed to locate the hook-wire commonly used for breast-conserving surgery in stage I and stage II cancer for nonpalpable lesions. A method to calculate the three-dimensional location of the tip of the hook-wire using the induced magnetic field strength data of the hook-wire was established. Numerical and experimental results revealed that the location of the tip of the hook-wire could be successfully estimated with the maximum error of 14.1 mm. This effective algorithm for locating the hook-wire can allow surgeons to remove the tissue containing the hook-wire accurately during procedure.

ACKNOWLEDGMENT

This work was supported by the MEXT Quantum Leap Flagship Program (MEXT Q-LEAP), Grant Numbers JPMXS0118067395 and JPMXS0118068379.

REFERENCE

- ¹ Nothacker M, Duda V, Hahn M, Warm M, Degenhardt F, Madjar H, Weinbrenner S, Albert U (2009), "Early detection of breast cancer: benefits and risks of supplemental breast ultrasound in asymptomatic women with mammographically dense breast tissue. A systemic review," BMC Cancer, 2009, 9–335.
- ² Sebastian M, Akbari S, Anglin B, Alice P (2015), "The impact of use of an intraoperative margin assessment device on re-excision rates," Springerplus, 4–198.
- ³ Thanasitthichai S, Chaiwerawattana A, Phadhana O (2016), "Impact of using intra-operative ultrasound guided breast conserving surgery on positive margin and re-excision rates in breast cancer cases with current SSO/ASTRO guidelines," APJCP, vol. 17, 4463–4467.
- ⁴ Elvecrog E, Lechner M, Nelson M (1993), "Nonpalpable Breast Lesions: Correlation of Stereotaxic Large Core Needle Biopsy and Surgical Biopsy Results" in Radiology, vol. 188, no. 2.

This is the author's peer reviewed, accepted manuscript. However, the online version of record will be different from this version once it has been copyedited and typeset.

PLEASE CITE THIS ARTICLE AS DOI: 10.1063/1.5000799

- ⁵ Peek MCL, Zada A, Ahmed M, Baker R, Sekino M, Kusakabe M, Douek M (2018), "Feasibility study evaluating a magnetic marker in an ex-vivo porcine model," *J. Magn. Mater.*, vol. 460, 334–339.
- ⁶ Xiao Y, Debnath O B, Chikaki S, Kuwahata A, Peek M, Saito I, Maeda S, Kusakabe M, Sekino M (2020) "Magnetic characteristics of a magnetic marker for localized tumor excision with a handheld magnetic probe," *AIP Adv.*, vol. 10, 1–5.
- ⁷ Maloney B W, McClatchy D M, Pogue B W, Paulsen K D, Wells W A, Barth R J (2018), "Review of methods for intraoperative margin detection for breast conserving surgery," *J. Biomed. Opt.*, vol. 23, 1–19.
- ⁸ Ookubo T, Inoue Y, Kim D, Ohsaki H, Mashiko Y, Kusakabe M, Sekino M (2013), "Characteristics of Magnetic Probes for identifying Sentinel Lymph Nodes," *Conf. Proc. IEEE Eng. Med. Biol. Soc.*, 5485–5488.
- ⁹ Sekino M, Kuwahata A, Ookubo T, Shiozawa M, Ohashi K, Kaneko M, Saito I, Inoue Y, Ohsaki H, Takei H, Kusakabe M (2018), "Handheld Magnetic Probe with Permanent Magnet and Hall Sensor for identifying Sentinel Lymph Nodes in Breast Cancer Patients" *Sci. Rep.* 8.
- ¹⁰ Louis K. Arate (1995), *Graphics Gem V* 1st ed., - chapter III.3- Trilinear Interpolation", 1st ed., Academic Press, 107–110.
- ¹¹ Kurita T, Taruno K, Nakamura S, Takei H, Enokido K, Kuwayama T, Kanada Y, Akashi-Tanaka S, Matsuyanagi M, Hankyo M, Yanagihara K, Sakatani T, Sakamaki K, Kuwahata A, Sekino M, Kusakabe M (2021), "Magnetically Guided Localization Using a Guiding-Marker System® and a Handheld Magnetic Probe for Nonpalpable Breast Lesions: A Multicenter Feasibility Study in Japan," *Cancers*, 13, 2923.